[1–3]. After the Chinese reports, the pilot and multicenter studies of ATO were conducted in the United States in relapsed or refractory APL patients. Combining the results from the pilot and multicenter studies, the CR rate was 87% [4, 5]. At present, ATO is the first-choice treatment of relapsed or refractory APL. In Japan, we have previously reported the prospective study of ATO in APL patients [6]. ATO was administered by the same protocol used in the United States multicenter study [5] to 14 relapsed APL patients who had not responded to ATRA and conventional chemotherapy, and of these 11 (78%) achieved CR.

While the clinical effect of ATO against APL was established, its pharmacokinetics has yet to be clarified. ATO is methylated by methyl transferase in the liver to monomethyl and dimethyl arsenic compounds, including the major metabolites monomethylarsonic acid (MAA^V) and dimethylarsinic acid ($DMAA^V$), which are mostly excreted into urine [7, 8]. Recent investigation shows that, among inorganic arsenic and methylated metabolites, As^{III} could induce cytotoxity against NB4 cells that derived from APL, degradation of PML-RARα chimeric protein that formed as a consequence of the t (15; 17) and causes the pathogenesis of APL, and differentiation in NB4 cells [9]. However, in most reports on the pharmacokinetics of ATO to patients with APL and other hematological malignancies, the arsenic concentrations were measured as total arsenic including metabolites [3, 10–14]. Recently, since the HPLC/ICP-MS, which combines high performance liquid chromatography (HPLC) and inductivity coupled plasma mass spectrometry (ICP-MS), was used for the quantitation of arsenic, the pharmacokinetics of arsenic species has been analyzed in several reports [15, 16]. However, the pharmacokinetic data of arsenic species for Asian people are presently limited [16].

In the prospective study [6], we have collected the blood and urine from 12 APL patients, subsequently stored frozen. Using the freeze-stored samples, we determined inorganic arsenic (As^{III} and As^V) and the major metabolites MAA^V and $DMAA^V$ concentrations by the HPLC/ICP-MS method [16], and conducted a pharmacokinetic analysis.

Patients and methods

Patients and administration schedule

The prospective study [6] was conducted at the Hamamatsu University School of Medicine in 14 APL patients from March 1999 to March 2001 according to the United States multicenter study [5]. ATO (Trisenox®) was provided by PolaRx Biopharmaceuticals (New York, NY, USA) and later from Cell Therapeutics (Seattle, WA, USA). Eligibility criteria and treatment plan were previously described. [6] The protocol was reviewed and approved by the institutional review board of the Hamamatsu University Hospital. Written informed consent was obtained from patients before the treatment. During the induction treatment, ATO was administered intravenously over 2 h at a dose of 0.15 mg/kg in 500 ml of 5% of dextrose given once daily for cumulative maximum of 60 days. Patients who had achieved complete remission received one course of consolidation therapy with ATO for a cumulative total of 25 days, using the same dose and schedule as the induction therapy.

Samples used in the pharmacokinetic analysis

The blood and urine were collected from 12 patients during the induction treatment. Samples were also collected from two patients (patient 7 and 9) during the consolidation treatment. Sample of blood of 5 ml was collected on the first day of administration (day 1) and after 1, 2, and 4 weeks from the start of administration. The time points for blood collection were as follows. On day 1 and after 4 weeks: before administration, 1 h, at the end of the infusion, 4, 6, 12 (or 18) and 24 h after the start of administration. After 1 and 2 weeks: before administration, at the end of the infusion, and 4 h after the start of administration.

The urine was collected for 24 h on day 1, and after 1, 2, and 4 weeks. After each urine sample collection, urine volume was measured. The plasma obtained from blood and urine samples were stored frozen (–20 or –80°C) until analysis.

As the standard arsenic compounds, sodium arsenite (As^{III}), sodium arsenate (As^V), monomethylarsonic acid (MAA^V), dimethylarsinic acid ($DMAA^V$), trimethyl arsenoxide (TMAsO), arsenobetaine (AB), arsenocholine (AsCho), tetramethylarsonium (TetMAs) and arseno-sugar (AsS) were purchased from Tri Chemical Laboratories Inc. (Yamanashi, Japan).

HPLC/ICP–MS analysis

The quantification of arsenic was performed by HPLC/ICP–MS, which combines HPLC (LC PU611 VS GL Sciences Inc., Tokyo, Japan) and ICP-MS (ELAN DRC-*e* Perkin Elmer SCIEX Inc., Ontario, Canada). [16] Inertsil AS (150 mm × 2.1 mm, 3.0 mm; GL Sciences Inc.) was used as the HPLC column and an

ODS guard column (GL Sciences Inc.) was attached to allow direct injection of the biological samples. Plasma samples were prepared using a protein precipitation procedure with acetonitrile. Urine samples were diluted twice with column eluate (dilution factor = 1:1). Column eluate was developed with 10 mM sodium butanesulfonate, 4 mM tetramethyl ammonium hydroxide, 4 mM malonic acid, and 0.05% methanol at pH 3.0 with HNO_3 and the elution flow rate used was 0.2 ml/min. All samples were filtered using a 0.45 μm membrane filter before injection.

The arsenic detection was performed at *m/z* 75 by ICP-MS. Sample solution of 5 μl was injected onto the guard column and the amount of each arsenic compound was obtained from the calibration curve (the standard arsenic compound was diluted with water to 1, 5, 10, and 20 ppb As). The lower limit of quantification for each arsenic species (As^{III}, As^{V} and the methylated metabolites) was 0.1 ppb.

Pharmacokinetic analysis

On the basis of plasma concentrations, the following pharmacokinetic parameters were calculated by non-compartmental analysis. It was not possible to calculate the parameters in some patients due to incomplete blood sampling. For inorganic arsenic, the parameters on day 1 were obtained from 10–11 patients and those on week 4 obtained from six patients. For the methylated metabolites, the C_{max} and T_{max} were obtained from 11–12 patients and $AUC_{0-tlast}$ was obtained from 9 patients on day 1 while these parameters were determined in six patients on week 4.

1. Maximum concentration (C_{max}) and time to reach C_{max} (T_{max}): C_{max} and T_{max} were obtained from the measured values.
2. Elimination rate constant (λz): λz was obtained by linear regression of the linear part of the log plasma concentration-time curve in the elimination phase according to the least squares method. The data points (≥ 3 time points) were used to perform linear regression and the slope of the fitted line with the best correlation coefficient was used as the elimination rate constant.
3. Elimination half-life ($t_{1/2,\beta}$): $t_{1/2,\beta}$ was calculated as $Ln(2)/\lambda z$.
4. Area under the plasma concentration-time curve (AUC): the AUC up to the final measurable time point (t_{last}) was calculated by the trapezoidal method ($AUC_{0-tlast}$) and added to $C_{tlast}/\lambda z$ to calculate $AUC_{0-\infty}$, where C_{tlast} is the concentration at t_{last}.
5. Total clearance (CL_{tot}): CL_{tot} was calculated as dose/$AUC_{0-\infty}$ on day 1 or dose/$AUC_{0-tlast}$ on week 4.
6. Volume of distribution (Vz, Vss): Vz was calculated from dose/($\lambda z \times AUC_{0-\infty}$) and Vss from dose × MRT/$AUC_{0-\infty}$. The $AUMC_{0-tlast}$ up to t_{last} ($= \int_0^t t \times Cdt$) was calculated by the trapezoidal method and added to $Ct/kel^2 + Ct \times t/kel$ to calculate $AUMC_{0-\infty}$ and MRT was obtained from $AUMC_{0-\infty}/AUC_{0-\infty}$.

On the basis of urinary concentrations, the urinary excretion (% of dose) and the renal clearance (CL_{re}) were calculated from the following equations:

$$\text{Urinary excretion (\%)} = \frac{\text{Urinary concentration } (\mu g/ml) \times \text{Total volume (ml)}}{\text{Dose } (\mu g/\text{body})} \times 100$$

$$\text{Renal clearance (l/kg h)} = \frac{\text{Urinary excretion } (\mu g)/\text{body weight (kg)}}{\text{AUC (ng h/ml)}}$$

WinNonlin standard version 4.1 (Pharsight Co., Palo Alto, CA, USA) was used for the non-compartmental analysis. Other calculations were performed using Microsoft Excel 2000 (Microsoft Co., Redmond, WA, USA).

Results

Patient background and efficacy results

The background and outcomes of ATO therapy for 12 APL patients are shown in Table 1. Ten of 12 patients achieved complete remission. Six of 10 patients who achieved CR became negative in the post-treatment RT-PCR test. Patient 11 died of

Table 1 Patient background and efficacy results

Patient number	Age	Sex	As_2O_3 treatment (days)		Outcome	RT-PCR for PML-RARα[b]	CR duration (month)
			Induction	Consolidation			
1	36	F	54	25	CR	–	22+
2	61	M	40	25	CR	–	10
3	36	F	46	20	CR	–	12+
4	33	F	41	25	CR	–	12+
5	58	M	41	25	CR	–	9+
6	52	M	43	–	CR	+	6
7	57	M	43	25	CR	+	12
8	23	F	27	25	CR	–	8
9	62	M	60	25	CR	+	8
10	50	M	44	–	CR	ND	4
11	65	M	21	–	Early death[a]	NA	–
12	64	M	64	–	NR	NA	–

ND not done; *NA* not applicable; *CR* complete remission; *NR* no response

[a] Due to cerebral hemorrhage on day 21

[b] Reverse transcriptase (RT)-PCR assays of bone marrow mononuclear cells for PML-RARα were performed after the consolidation treatment

cerebral hemorrhage on day 21, and patient 12 was discontinued the administration on day 92 because ATO was ineffective.

For two patients (patient 7 and 8) the blood and urine were collected also during the consolidation treatment.

Pharmacokinetics of arsenic species on the first day of administration

The plasma concentrations of inorganic arsenic (As^{III} and As^{V}) on day 1 are shown in Fig. 1, and the pharmacokinetic parameters in Table 2. The plasma concentration of As^{III} reached C_{max} immediately after the administration in most of the patients, followed by a biphasic decline with a mean $t_{1/2,\beta}$ of 17 h after an initial distribution phase (up to 4–8 h after the start of administration). The mean C_{max} was 12.4 ± 8.4 ng/ml. The mean volume of distribution at steady state (Vss) was large (55.9 l/kg) suggesting extensive distribution throughout the body. The plasma concentration profile of As^{V} was similar to that of As^{III}. After reaching C_{max} of 10.2 ± 3.9 ng/ml, a biphasic decline was observed with a mean $t_{1/2,\beta}$ of 18.3 h. After the end of the infusion, the As^{V} plasma concentrations initially declined more slowly than those for As^{III}, and hence the $AUC_{0-\infty}$ of As^{V} was about twice that of As^{III} (As^{III}, 80.5 ± 39.8 ng h/ml; As^{V}, 155.1 ± 78.6 ng h/ml). In addition, the pharmacokinetic parameters for the inorganic arsenic concentrations (the total measured As^{III} and As^{V} values) were calculated, and the results indicated a C_{max} of 22.6 ± 11.4 ng/ml and $AUC_{0-\infty}$ of 211.8 ± 55.1 ng h/ml.

The plasma concentrations and the pharmacokinetic parameters of major metabolites (MAA^{V}, $DMAA^{V}$) on day 1 are shown in Fig. 2 and Table 2, being compared to the inorganic arsenic (As^{III} + As^{V}). The MAA^{V} and $DMAA^{V}$ concentrations were below the quantification limit until immediately after completion of administration, but a gradual increase was observed from 4 h after the start of administration reaching C_{max} in many patients at 24 h after administration, the final time point on day 1. The mean C_{max} values were 3.1 ± 1.6 and 5.4 ± 2.9 ng/ml, respectively. The plasma concentrations of arsenobetaine (AB), an organic

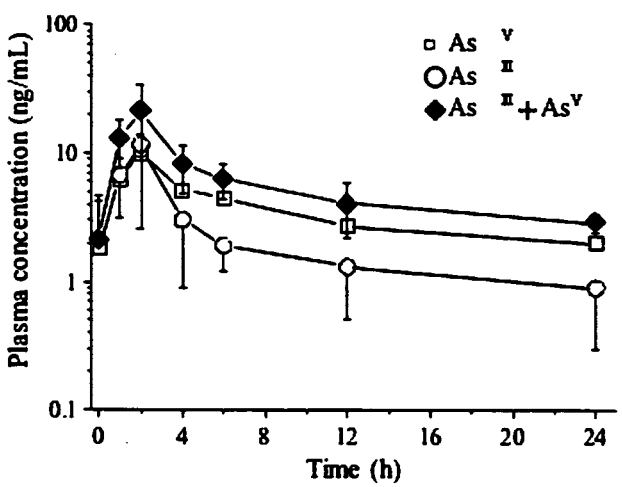

Fig. 1 Plasma concentrations of inorganic arsenic on day 1 of the repeated administration. The values shown in the figure were determined in 12 patients (N = 14; mean ± standard deviation). The values obtained during the induction and consolidation treatment were used for patient 7 and 8

Table 2 Pharmacokinetic parameters of inorganic arsenic (As^{III} + As^{V}) and its metabolites (MAA^{V}, $DMAA^{V}$) on day 1 and week 4

Arsenic species	Day		T_{max} (h)	C_{max} (ng/ml)	$t_{1/2,\beta}$ (h^{-1})	$AUC_{0-tlast}$ (ng h/ml)	$AUC_{0-\infty}$ (ng h/ml)	Vz (l/kg)	CLtot (l/kg/h)	Vss (l/kg)
Inorganic Arsenic[a] As^{III}+As^{V}	Day 1	Mean	1.9	22.6	15.4	138.6	211.8	15.2	0.7	14.3
		SD	0.7	11.4	9.2	32.4	55.1	6.7	0.2	6.3
	Week 4	Mean	2.0	23.2	24.2	233.3	474.8	12.8	0.8	12.5
		SD	0.3	10.2	12.5	92.8	192.6	10.6	0.5	10.4
As^{IIIa}	Day 1	Mean	1.9	12.4	17.0	52.8	80.5	44.0	2.3	55.9
		SD	0.7	8.4	19.0	21.2	39.8	27.5	1.3	55.9
	Week 4	Mean	1.6	10.1	24.8	82.6	190.6	41.5	2.7	39.7
		SD	0.5	6.6	12.3	55.7	189.9	28.6	1.7	28.1
As^{Vb}	Day 1	Mean	1.8	10.2	18.3	86.9	155.1	25.8	1.2	24.8
		SD	0.9	3.9	11.3	22.5	78.6	9.4	0.6	8.9
	Week 4	Mean	2.0	14.2	32.2	150.7	357.5	21.0	1.2	20.6
		SD	0.3	6.6	24.2	51.9	164.7	18.6	0.8	18.4
MAA^{Vc}	Day 1	Mean	18.0	3.1	–	48.7	–	–	–	–
		SD	6.4	1.6	–	12.9	–	–	–	–
	Week 4	Mean	3.9	10.9	–	174.2	–	–	–	–
		SD	6.5	4.7	–	66.1	–	–	–	–
$DMAA^{Vd}$	Day 1	Mean	20.1	5.4	–	83.1	–	–	–	–
		SD	6.3	2.9	–	30.8	–	–	–	–
	Week 4	Mean	5.6	21.4	–	374.1	–	–	–	–
		SD	9.2	12.3	–	214.5	–	–	–	–

– Not analyzable

T_{max} time to maximum concentration, C_{max} maximum concentration, $t_{1/2,\beta}$ apparent terminal half-life, $AUC_{0-tlast}$ area under the curve from time zero to the final measurable time point (t_{last}), $AUC_{0-\infty}$ area under the curve from time zero to infinity, Vz volume of distribution at the terminal phase, CL_{tot} systemic clearance, Vss volume of distribution at steady-state

The values obtained during the induction and consolidation treatment were used for patient 7, while the values obtained during the consolidation treatment were used for patient 8

[a] The values obtained from ten patients (N = 11) on day 1 and six patients (N=6) in week 4 were analyzed

[b] The values obtained from 11 patients (N = 12) on day 1 and six patients (N=6) in week 4 were analyzed

[c] The C_{max} and T_{max} were obtained from 12 patients (N=13) and $AUC_{0-tlast}$ was obtained from 9 patients (N=10) on day 1 while these parameters were determined in six patients (N=6) in week 4

[d] The C_{max} and T_{max} were obtained from 11 patients (N=12) and $AUC_{0-tlast}$ was obtained from 9 patients (N=10) on day 1 while these parameters were determined in six patients (N=6) in week 4

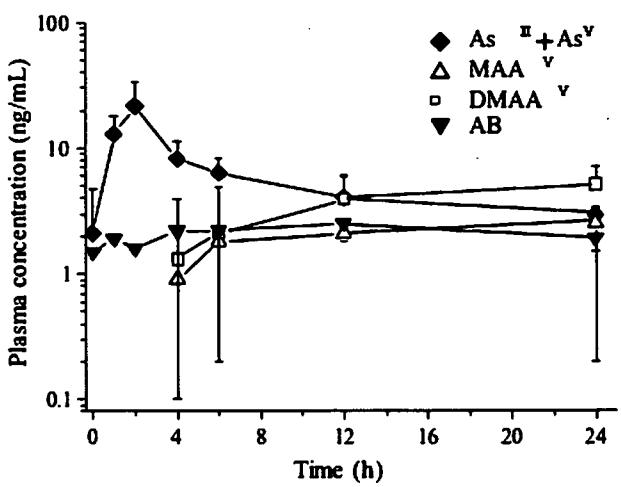

Fig. 2 Plasma concentrations of inorganic arsenic and methylated metabolites (MAA^{V}, $DMAA^{V}$, AB) on day 1 of the repeated administration. The values shown in the figure were determined in 12 patients (N = 14; mean ± standard deviation). The values obtained during the induction and consolidation treatment were used for patient 7 and 8

arsenic compound derived from seafood, remained almost constant (about 2 ng/ml) during the study period. Accordingly, the influence of arsenic derived from meals in this study was considered negligible.

For the 2 patients (patient 7 and 8) whose arsenic concentrations were determined both the induction and consolidation treatment, the plasma concentrations of As^{III}, As^{V}, and MAA^{V} had decreased below the quantitation limit during the washout period (69 days for patient 7; 37 days for patient 8) before the consolidation treatment, and only the $DMAA^{V}$ concentration of 1.9 ng/ml was detected in patient 8. For patient 7, the blood was collected 9 days after the completion of the induction treatment for 43 days receiving a total of 448 mg ATO, and the plasma concentrations were as follows: As^{V}—0, As^{III}—0, MAA^{V}—1.9 ng/ml, $DMAA^{V}$—8.3 ng/ml, indicating the complete disappearance of inorganic arsenic. These results indicate that most of the inorganic arsenic is

promptly metabolized to $DMAA^V$ and ATO is not accumulated in the blood.

Pharmacokinetics of arsenic species during the repeated administration

The mean plasma concentrations of inorganic arsenic ($As^{III} + As^V$) and its metabolites (MAA^V and $DMAA^V$) on day 1 and weeks 1, 2, and 4 during the repeated administration are shown in Fig. 3, and the pharmacokinetic parameters on day 1 and week 4 are in Table 2. In comparison with the levels on day 1, the C_{max} of inorganic arsenic on week 4 was similar but the elimination was delayed. As a result, the $AUC_{0-\infty}$ increased about twofold. However, the $AUC_{0-tlast}$ of inorganic arsenic on week 4 was similar to the $AUC_{0-\infty}$ on day 1, indicating that no marked change was observed in CL_{tot} during the repeated administration. The mean concentration profile from day 1 to week 4 indicated no increase in the C_{max} of inorganic arsenic related to administration frequency. These results suggest that the plasma concentration had reached the steady state. Alternatively, the plasma concentrations of MAA^V and $DMAA^V$ increased along with the increase in administration frequency during the repeated administration. The C_{max} and $AUC_{0-tlast}$ of both metabolites on week 4 were about four times those of the respective levels observed on day 1. The plasma concentrations of AB remained almost constant (about 2–4 ng/ml) during the repeated administration.

Urinary excretions of arsenic species

The urinary excretions (daily excretion rate, % of dose) of inorganic arsenic and methylated metabolites on day 1 and weeks 1, 2, and 4 during the repeated administration are shown in Table 3. The respective excretions of As^{III} and As^V on day 1 accounted for about 6%. During the repeated administration, the excretions increased and remained almost constant after week 1–4 (As^{III}: about 13–16%, As^V: about 7–8%), suggesting that the steady state was attained. A similar tendency was observed in the excretion rates of MAA^V and $DMAA^V$ on day 1 and during the repeated administration. The mean total arsenic excretion rate including inorganic arsenic and methylated arsenic was about 20% of daily dose on day1 and remained at about 60% of daily dose during week 1–4.

The CL_{re} values for As^{III} and As^V were about 10 and 6% of the CL_{tot} (shown in Table 2), respectively. These results indicate that renal excretion play no significant role in the elimination of inorganic arsenic, and suggest that hepatic elimination appears to be the main route of systemic clearance.

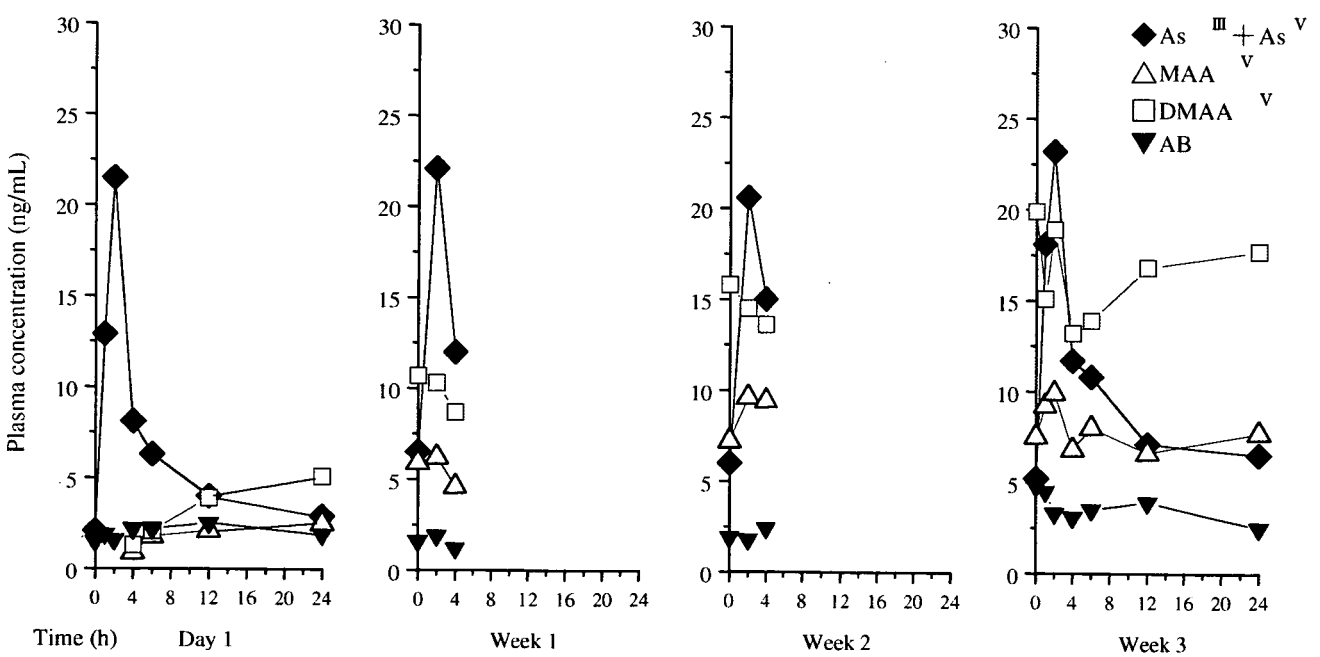

Fig. 3 The plasma concentrations of inorganic arsenic ($As^{III} + As^V$) and its metabolites (MAA^V, $DMAA^V$, and AB) on day 1 and weeks 1, 2, and 4. The values shown in the figure indicate mean values determined in 12 patients ($N = 14$) on day 1, in nine patients ($N = 10$) during week 1, in ten patients ($N = 12$) during week 2 and in seven patients ($N = 7$) during week 4. The values obtained in the induction and consolidation treatment were used for patients 7 and 8

Table 3 Urinary excretions of inorganic arsenic and methylated metabolites during the repeated administration

		Urinary excretions (% of dose)				CLre (l/kg/h)	
		Day 1	Week 1	Week 2	Week 4	Day 1	Week 4
As^{III}	Mean	6.5	16.2	12.8	13.7	0.20	0.32
	SD	4.9	10.1	8.3	9.6	0.10	0.14
As^{V}	Mean	5.6	7.3	8.2	6.8	0.07	0.07
	SD	5.9	8.6	12.1	8.2	0.06	0.06
MAA^{V}	Mean	5.0	17.4	12.9	19.6	0.11	0.17
	SD	2.5	11.2	5.9	10.0	0.07	0.10
$DMAA^{V}$	Mean	3.2	19.4	19.8	21.1	0.05	0.10
	SD	1.3	8.5	9.6	9.5	0.03	0.03
Total	Mean	20.4	60.3	53.7	61.1	–	–
	SD	7.4	25.1	22.6	28.5	–	–

The urine was collected for 24 h on each measurement day. The values obtained during the induction and consolidation treatment were used for patient 7 and 8. The urine samples obtained from nine patients (N = 11) on day 1, from nine patients (N = 10) during week 1, from nine patients (N = 11) during week 2 and from six patients (N = 6) during week 4 were analyzed

CL_{re} values were obtained from five to seven patients (N = 6–8) on day 1 and from four to five patients (N = 4–5) on week 4

Discussion

The plasma and urine concentrations of inorganic arsenic and methylated metabolites in APL patients treated with ATO were determined with HPLC/ICP–MS to clarify the pharmacokinetics of arsenic species. Until recently, arsenic was determined as the total arsenic content including metabolites in most of the reports on the pharmacokinetics of ATO. The current report therefore has considerable clinical meaning because it is the first study investigating the pharmacokinetics of arsenic species in as many as 12 Japanese patients with APL.

Arsenic is contained in foods and especially abundant in fish, shellfish, and seaweed. Arsenic compounds abundant in seafood are mainly organic such as arsenobetaine (AB), a trimethylarsenic compound. The toxicity of AB is extremely low and it is quickly excreted unmetabolized [17, 18]. Since the Japanese people ingest a large quantity of seafood, their urinary concentration of arsenic is higher as an ethnic characteristic. Then the influence of AB derived from meals cannot be ignored, especially for the Japanese. It is possible to determine AB separately from other arsenic compounds in plasma and urine by HPLC/ICP-MS. Therefore this method is very effective to analyze the pharmacokinetics of arsenic species in the Japanese APL patients.

In our study, As^{V} was detected in the plasma and urine at a concentration equivalent to or higher than that of As^{III} and the pharmacokinetic parameters of inorganic arsenic (As^{III} + As^{V}) were similar to those of As^{III} in the Westeners. [Remick et al. J Clin Oncol 2004; 22:2018 (abstract)]. The previous reports have shown that the As^{V} concentrations in plasma or urine after ATO administration are very low. [15, 16, 19] The conversion from As^{III} to As^{V} occurs as natural oxidation while arsenate reductase mainly contributes to the reduction from As^{V} to As^{III} [20]. In general, the pentavalent arsenic compound is more stable than the trivalent arsenic compound. Feldmann et al. [21] reported that As^{III}, As^{V}, MAA^{V}, and $DMAA^{V}$ remained stable up to 2 months in human urine at 4°C or –20°C, but that about 30% of As^{III} was oxidized to As^{V} in some urine samples after storage at 4°C for longer than 4 months. Del Razo et al. [22] analyzed the stability of arsenic compound in aqueous solution and urine at 4°C and reported that 20 and 21–32% of As^{III} were oxidized, respectively after 2 months. Considering that the plasma and urine samples analyzed in our study were stored frozen for about 5 years, it is highly likely that the As^{V} in the plasma and urine was generated by oxidation of As^{III} during the storage period.

During the repeated administration, the plasma concentrations of inorganic arsenic reached the steady state, whereas accumulation of MAA^{V} and $DMAA^{V}$ in the blood was related to administration frequency. These accumulations were observed also in the Westerners. The total arsenic concentrations reported previously [11, 12, 14] indicated a tendency to increase during the repeated administration of ATO to patients with APL and other hematological malignancies. The results obtained in our study, indicate most of the increase in the total arsenic concentrations can be attributed to the accumulation of methylated metabolites.

During the repeated administration, approximately 60% of the administered arsenic trioxide dose was

excreted in urine as inorganic arsenic and methylated species in Japanese patients. There was not marked difference in the urinary excretions of inorganic arsenic ($As^{III} + As^{V}$) between the Westerners and the Japanese. These results were similar to those in the reports for the excretion of arsenic in humans [15, 23, 24]. In addition, CL_{re} was much lower than CL_{tot} for inorganic arsenic, indicating that renal excretion plays no significant role in the elimination of inorganic arsenic. It is therefore considered that the plasma concentrations of inorganic arsenic do not increase in patients with impaired renal function, as shown by Remick et al. [J Clin Oncol 2004; 22:2018 (abstract)] These results suggest that there were no marked differences in the plasma profiles and urinary excretions of inorganic arsenic and methylated metabolites during the repeated administration of ATO between the Westerners and the Japanese APL patients.

The problem that should be considered when treating APL patients with ATO is chronic arsenic poisoning which is induced by the intratracheal and oral exposure to a comparatively small amount of arsenic for a long term (ten or more years). The symptoms demonstrated in chronic arsenic poisoning are disorders in the skin, mucosa, peripheral nerves, liver, and respiratory organs as well as skin and lung cancer. According to the previous reports, the total arsenic concentrations in the blood of inhabitants who drank well water contaminated with arsenic (5–410 ng/ml) were 2–42.1 ng/ml [25]. These results are similar to the plasma concentrations in this study. Though the liver function abnormalities and peripheral neuropathies occurred in patients of this study [6], they have improved after completion of administration. In the case of treatment for APL, the administration of ATO is not continued permanently or long-term and arsenic is promptly excreted during the washout period. Therefore, it is unlikely that the treatment with ATO results in chronic arsenic poisoning, although sufficient attention should be paid to the adverse reactions during the treatment.

In conclusion, the present study showed the pharmacokinetics of arsenic species in Japanese APL patients treated with ATO. The plasma concentrations of inorganic arsenic (As^{III} and As^{V}) reached the C_{max} immediately after completion of administration followed by a biphasic elimination. However, the appearance of methylated metabolites (MAA^{V}, $DMAA^{V}$) in the blood was delayed. During the repeated administration, the pharmacokinetics of inorganic arsenic reached the steady state but the concentrations of MAA^{V} and $DMAA^{V}$ increased in relation to administration frequency. ATO is metabolized when administered intravenously to APL patients and methylated metabolites are promptly eliminated from the blood and excreted into urine after completion of administration, consequently indicating no measurable accumulation of ATO in the blood. These results are considered important information for the current and future clinical use of ATO.

Acknowledgments We thank Mr. Masaya Tajima and Dr. Hideya Mukai from Nippon Shinyaku Co. Ltd. for their help in preparing this article.

Appendix

We express our sincere gratitude to Drs. Masahito Ishibashi (St. Marianna School of Medicine), Michio Ihara (Seirei Hamamatsu Hospital), Hiroshi Yamazaki (Kumamoto City Hospital), Fumio Kawano (National Kumamoto Hospital), Kou Tanaka (Suzuka Kaisei General Hospital), Nobuhiko Emi (Nagoya University School of Medicine), Mitsuhiro Hashimoto (Nippon Medical School), Kazuteru Ohashi (Tokyo Metropolitan Komagome Hospital), Atsushi Taguchi, Katsumichi Fujimaki (Kanagawa Cancer Center), Noriyuki Hirabayashi (Nagoya Second Red-Cross Hospital), Hirotsugu Kojima (Fujita Health University School of Medicine), and Masao Tomonaga (Nagasaki University School of Medicine) for recruiting patients in this study.

References

1. Sun HD, Ma L, Hu XC, Zhang TD (1992) Ai-Lin I treated 32 cases of acute promyelocytic leukemia. Chin J Integr Chin and West Med 12:170–171
2. Zhang P, Wang SY, Hu LH (1996) Arsenic trioxide treated 72 cases of acute promyelocytic leukemia. Chin J Hematol 17:58–62
3. Shen ZX, Chen GQ, Ni JH, Li XS, Xiong SM, Qiu QY, Zhu J, Tang W, Sun GL, Yang KQ, Chen Y, Zhou L, Fang ZW, Wang YT, Ma J, Zhang P, Zhang TD, Chen SJ, Chen Z, Wang ZY (1997) Use of arsenic trioxide (As_2O_3) in the treatment of acute promyelocytic leukemia (APL): II. Clinical efficacy and pharmacokinetics in relapsed patients. Blood 89:3354–3360
4. Soignet SL, Maslak P, Wang ZG, Jhanwar S, Calleja E, Dardashti LJ, Corso D, DeBlasio A, Gabrilove J, Scheinberg DA, Pandolfi PP, Warrell RP Jr (1998) Complete remission after treatment of acute promyelocytic leukemia with arsenic trioxide. N Engl J Med 339:1341–1348
5. Soignet SL, Frankel SR, Douer D, Tallman MS, Kantarjian H, Calleja E, Stone RM, Kalaycio M, Scheinberg DA, Steinherz P, Sievers EL, Coutre S, Dahlberg S, Ellison R, Warrell RP Jr (2001) United States multicenter study of arsenic trioxide in relapsed acute promyelocytic leukemia. J Clin Oncol 19:3852–3860

6. Ohnishi K, Yoshida H, Shigeno K, Nakamura S, Fujisawa S, Naito K, Shinjo K, Fujita Y, Matsui H, Sahara N, Takeshita A, Satoh H, Terada H, Ohno R (2002) Arsenic trioxide therapy for relapsed or refractory Japanese patients with acute promyelocytic leukemia: need for careful electrocardiogram monitoring. Leukemia 16:617–622
7. Challenger F (1945) Biological methylation. Chem Rev 36:315–361
8. Cullen W. R, Reimer K. J (1989) Arsenic speciation in the environment. Chem Rev 89:713–764
9. Chen GQ, Zhou L, Styblo M, Walton F, Jing Y, Weinberg R, Chen Z, Waxman S (2003) Methylated metabolites of arsenic trioxide are more potent than arsenic trioxide as apoptotic but not differentiation inducers in leukemia and lymphoma cells. Cancer Res 63:1853–1859
10. Shen Y, Shen ZX, Yan H, Chen J, Zeng XY, Li JM, Li XS, Wu W, Xiong SM, Zhao WL, Tang W, Wu F, Liu YF, Niu C, Wang ZY, Chen SJ, Chen Z (2001) Studies on the clinical efficacy and pharmacokinetics of low-dose arsenic trioxide in the treatment of relapsed acute promyelocytic leukemia: a comparison with conventional dosage. Leukemia 15:735–741
11. Raffoux E, Rousselot P, Poupon J, Daniel MT, Cassinat B, Delarue R, Taksin AL, Rea D, Buzyn A, Tibi A, Lebbe G, Cimerman P, Chomienne C, Fermand JP, de The H, Degos L, Hermine O, Dombret H (2003) Combined treatment with arsenic trioxide and all-trans-retinoic acid in patients with relapsed acute promyelocytic leukemia. J Clin Oncol 21:2326–2334
12. Rousselot P, Larghero J, Arnulf B, Poupon J, Royer B, Tibi A, Madelaine-Chambrin I, Cimerman P, Chevret S, Hermine O, Dombret H, Claude Brouet J, Paul Fermand J (2004) A clinical and pharmacological study of arsenic trioxide in advanced multiple myeloma patients. Leukemia 18:1518–1521
13. Ishitsuka K, Shirahashi A, Iwao Y, Shishime M, Takamatsu Y, Takatsuka Y, Utsunomiya A, Suzumiya J, Hara S, Tamura K (2004) Bone marrow necrosis in a patient with acute promyelocytic leukemia during re-induction therapy with arsenic trioxide. Eur J Haematol 72:280–284
14. Westervelt P, Brown RA, Adkins DR, Khoury H, Curtin P, Hurd D, Luger SM, Ma MK, Ley TJ, DiPersio JF (2001) Sudden death among patients with acute promyelocytic leukemia treated with arsenic trioxide. Blood 98:266–271
15. Wang Z, Zhou J, Lu X, Gong Z, Le XC (2004) Arsenic speciation in urine from acute promyelocytic leukemia patients undergoing arsenic trioxide treatment. Chem Res Toxicol 17:95–103
16. Fukai Y, Hirata M, Ueno M, Ichikawa N, Kobayashi H, Saitoh H, Sakurai T, Kinoshita K, Kaise T, Ohta S (2006) Clinical pharmacokinetic study of arsenic trioxide in an acute promyelocytic leukemia (APL) patients: speciation of arsenic metabolites in serum and urine. Biol Pharm Bull 29:1022–1027
17. Kaise T,Watanabe S, Itoh K (1985) The acute toxicity of arsenobetaine. Chemosphere 14:1327–1332
18. Yamauchi H, Yamamura Y (1984) Metabolism and excretion of orally ingested trimethyl arsenic in man. Bull Environ Contam Toxicol 32:682–687
19. Benramdane L, Accominotti M, Fanton L, Malicier D, Vallon JJ (1999) Arsenic speciation in human organs following fatal arsenic trioxide poisoning—a case report. Clin Chem 45:301–306
20. Vasken Aposhian H, Zakharyan RA, Avram MD, Sampayo-Reyes A, Wollenberg ML (2004) A review of the enzymology of arsenic metabolism and a new potential role of hydrogen peroxide in the detoxication of the trivalent arsenic species. Toxicol Appl Pharmacol 198:327–335
21. Feldmann J, Lai VW, Cullen WR, Ma M, Lu X, Le XC (1999) Sample preparation and storage can change arsenic speciation in human urine. Clin Chem 45:1988–1997
22. Del Razo LM, Styblo M, Cullen WR, Thomas DJ (2001) Determination of trivalent methylated arsenicals in biological matrices. Toxicol Appl Pharmacol 174:282–293
23. Pomroy C, Charbonneau SM, McCullough RS, Tam GK (1980) Human retention studies with ^{74}As. Toxicol Appl Pharmacol 53:550–556
24. Buchet.JP, Lauwerys R, Roels H (1981) Urinary excretion of inorganic arsenic and its metabolites after repeated ingestion of sodium meta-arsenite by volunteers. Int Arch Occup Environ Health 48:111–118
25. Mandal BK, Ogra Y, Anzai K, Suzuki KT (2004) Speciation of arsenic in biological samples. Toxicol Appl Pharmacol 198:307–318

Oncogene (2007) 26, 4179–4188

www.nature.com/onc

ONCOGENOMICS

Identification and functional signature of genes regulated by structurally different ABL kinase inhibitors

K Nunoda[1], T Tauchi[1], T Takaku[1], S Okabe[1], D Akahane[1], G Sashida[1], JH Ohyashiki[2] and K Ohyashiki[1]

[1]*First Department of Internal Medicine, Tokyo Medical University, Shinjuku-ku, Tokyo, Japan and* [2]*Intractable Disease Research Center, Tokyo Medical University, Shinjuku-ku, Tokyo, Japan*

Dasatinib is an ATP-competitive, multi-targeted SRC and ABL kinase inhibitor that can bind BCR-ABL in both the active and inactive conformations. From a clinical standpoint, dasatinib is particularly attractive because it has been shown to induce hematologic and cytogenetic responses in imatinib-resistant chronic myeloid leukemia patients. The fact because the combination of imatinib and dasatinib shows the additive/synergistic growth inhibition on wild-type p210 BCR-ABL-expressing cells, we reasoned that these ABL kinase inhibitors might induce the different molecular pathways. To address this question, we used DNA microarrays to identify genes whose transcription was altered by imatinib and dasatinib. K562 cells were cultured with imatinib or dasatinib for 16 h, and gene expression data were obtained from three independent microarray hybridizations. Almost all of the imatinib- and dasatinib-responsive genes appeared to be similarly increased or decreased in K562 cells; however, small subsets of genes were identified as selectively altered expression by either imatinib or dasatinib. The distinct genes that are selectively modulated by dasatinib are cyclin-dependent kinase 2 (*CDK2*) and *CDK8*, which had a maximal reduction of <5-fold in microarray screen. To assess the functional importance of dasatinib regulated genes, we used RNA interference to determine whether reduction of *CDK2* and *CDK8* affected the growth inhibition. K562 and TF-1BCR-ABL cells, pretreated with *CDK2* or *CDK8* small interfering RNA, showed additive growth inhibition with imatinib, but not with dasatinib. These findings demonstrate that the additive/synergistic growth inhibition by imatinib and dasatinib may be mediated in part by *CDK2* and *CDK8*.
Oncogene (2007) **26,** 4179–4188; doi:10.1038/sj.onc.1210179; published online 8 January 2007

Keywords: BCR-ABL; tyrosine kinase inhibitor; imatinib; dasatinib

Correspondence: Dr T Tauchi, First Department of Internal Medicine, Tokyo Medical University, 6-7-1 Nishishinjuku, Shinjuku-ku, Tokyo 160-0023, Japan.
E-mail: tauchi@tokyo-med.ac.jp
Received 17 February 2006; revised 26 October 2006; accepted 27 October 2006; published online 8 January 2007

Introduction

SRC family kinases regulate multiple cellular events such as proliferation, differentiation, survival, cytoskeletal organization, adhesion and migration as a consequence of their ability to couple with many diverse classes of cellular receptors and many distinct cellular targets (Thomas and Brugge, 1997). SRC kinases are involved in BCR-ABL-mediated transformation and have been implicated in imatinib resistance (Donato *et al.*, 2003; Dai *et al.*, 2004). Multiple domains of BCR-ABL interact with and activate SRC kinases independently of BCR-ABL kinase activity (Warmuth *et al.*, 1997; Stanglmaier *et al.*, 2003). The studies with dominant-negative mutants suggest that SRC kinases may contribute to the proliferation and survival of myeloid cell lines expressing BCR-ABL *in vitro* (Lionberger *et al.*, 2000). HCK and LYN are expressed and activated in the acute phase of chronic myeloid leukemia (CML) patients, and their upregulation correlates with disease progression and resistance in patients with imatinib (Hofmann *et al.*, 2002; Donato *et al.*, 2003; Dai *et al.*, 2004; Ptasznik *et al.*, 2004). Therefore, dual SRC and ABL kinase inhibitors are attractive for the treatment of imatinib-resistant CML.

Dasatinib is an orally available multitargeted SRC and ABL kinase inhibitor with two-log increased potency relative to imatinib (Shah *et al.*, 2004). Mutations in BCR-ABL that favor the adoption of an active, imatinib-resistant conformation are effectively targeted by dasatinib, as shown in cell lines expressing 14 imatinib-resistant mutants (Shah *et al.*, 2004; Burgess *et al.*, 2005; O'Hare *et al.*, 2005). Dasatinib prolonged survival of mice with BCR-ABL-driven disease, and inhibited proliferation of BCR-ABL-positive bone marrow progenitor cells from patients with imatinib-sensitive or imatinib-resistant CML (Shah *et al.*, 2004). A recent saturation mutagenesis screening of BCR-ABL also found that the spectrum of mutations that would allow for dasatinib resistance is reduced compared with that of imatinib, including L248R, Q252H, E255K, V299L, T315I/A and F317V (Burgess *et al.*, 2005). Molecular docking studies also showed that dasatinib is likely to bind the inactive form of BCR-ABL, although requiring a lower conformational stringency, with the ability of binding more intermediate

conformations than imatinib (Gambacorti-Passerini *et al.*, 2005). From a clinical standpoint, dasatinib is particularly hopeful because it has been shown to induce hematologic and cytogenetic responses in imatinib-resistant CML patients (Talpaz *et al.*, 2006). The fact that because the combination of imatinib and dasatinib shows additive/synergistic growth inhibition on wild-type p210 BCR-ABL-expressing cells, we reasoned that these ABL kinase inhibitors might induce different molecular pathways. To address this question, we used DNA microarrays to identify genes whose transcription was altered by imatinib and dasatinib. The distinct genes that are selectively modulated by dasatinib are cyclin-dependent kinase 2 (*CDK2*) and *CDK8*. To assess the functional importance of dasatinib-regulated genes, we used RNA interference to determine whether reduction of *CDK2* and *CDK8* affected the growth inhibition. K562 and TF-1BCR-ABL cells, pretreated with *CDK2* or *CDK8* small interfering RNA (siRNA), showed additive growth inhibition with imatinib but not with dasatinib. These findings demonstrate that the additive growth inhibition by imatinib and dasatinib may be mediated by *CDK2* and *CDK8*.

Results

Analysis of combined drug effects

First, we investigated the combined use of dasatinib with the anti-leukemic agents imatinib, daunorubicin (DNR), AraC and VP16 *in vitro*. Previous study demonstrated that imatinib showed additive or synergistic effects in combination with some leukemic agents (Nakajima *et al.*, 2003). We therefore determined whether dasatinib could increase the effects of some anti-leukemic agents, including imatinib, in CML blastic crisis cell line K562. The concentration of anti-leukemic agents is plotted against percentage inhibition of proliferation, and each anti-leukemic agent alone is compared with each anti-leukemic agent in combination with 0.2 nM of dasatinib (Figure 1a). Regression lines generated by Microsoft Excel represent the best-fit relationship between drug concentration and the percentage inhibition of proliferation. R^2 values are the square of the correlation coefficient. When imatinib was combined with 0.2 nM of dasatinib, the curve showed a substantial shift downward, consistent with increased antiproliferative activity of the drug combination (Figure 1a). Similarly, with the combination of DNR or VP-16 and dasatinib, the curve also shifted down (Figure 1a). When AraC was combined with dasatinib, the two curves crossed at 500 nM of AraC (Figure 1a). There was no additive effect of the combination of AraC and dasatinib. Although dasatinib and imatinib bind to overlapping sites within the BCR-ABL kinase domain, the clinically available concentrations of imatinib may not exert an interfering effect by restricting the dasatinib's access to its binding site.

Next, we determined whether inhibition of BCR-ABL-tyrosine kinase by co-treatment with dasatinib and imatinib would attenuate the downstream molecules of BCR-ABL (Figure 1b–d). As compared with treatment with either agent alone, co-treatment with imatinib (0.5 μM) and dasatinib (5 nM) or imatinib (1.0 μM) and dasatinib (10 nM) for 24 h caused more inhibition of BCR-ABL autophosphorylation (Figure 1b). Combined treatment with imatinib and dasatinib also caused more attenuation of the levels of p-Akt, phosphor-nuclear factor kappa B (NF-κB) and c-Myc, which are downstream of BCR-ABL (Figure 1c and d).

Dasatinib and imatinib-induced gene expression profiles

K562 cells were cultured with dasatinib or imatinib for 16 h, and gene expression data from three independent microarray hybridizations were analysed (GPL 2523) (Figure 2a and b). The microarray experiment data were deposited in GEO (GSE 2810). Although the data in this result demonstrated genuine differential expression, most of these genes showed changes that were relatively small in magnitude. We, therefore, restricted to genes that showed at least a 1.5-fold change. Almost all of the dasatinib or imatinib responsible genes appeared to be similarly changed; however, small subsets of genes were identified as selectively altered in expression by either dasatinib or imatinib (Figures 3 and 4). In 16 h, 155 of the 667 unique dasatinib genes and 144 of the 667 unique imatinib genes were regulated >1.5-fold. This finding suggests that these two structurally diverse BCR-ABL tyrosine kinase inhibitors initially regulate highly overlapping common target genes and pathway. The common genes whose expression was affected by dasatinib and imatinib were categorized into different functional groups based on their biological function, and genes in the cell proliferation and apoptosis categories were examined in greater detail (Figures 3 and 4).

Cell proliferation-related genes

Dasatinib and imatinib affected the expression of several cyclin-dependent kinases (*CDK2*, *CDK4*, *CDC5R*, *CDK6* and *CDK8*), cell division cycle genes (*CDC2L5*, *CDC7*, *CDC25A* and *CDC25B*) and cyclines (*CCNA2*, *CCNC*, *CCND2*, *CCND3*, *CCNE1*, *CCNE2* and *CCNH*) (Figure 3a and b). These regulators are known to be involved in G1/S and G2/M transition, and their decreased gene expression levels and thus reduced activities are essential for cell cycle arrest at early stage. Dasatinib and imatinib also affected the expression of mitotic inhibitors (*CDKN1A*, *CDKN1B*, *CDKN1C*, *CDHN2C* and *CDK2AP1*) (Figure 3b). Obviously, downregulation/inactivation of such a large number of cell cycle-related genes may abolish the cell cycle machinery, probably a prerequisite for apoptosis in dasatinib- or imatinib-treated CML cells. The distinct genes that are selectively modulated by dasatinib are *CDK2* and *CDK8*, which had a maximal reduction of <5-fold in microarray screen. *CDK2* and *CDK8* appeared to be candidates involved in the additive/synergistic growth inhibition by dasatinib and imatinib. Downregulation of these genes can be largely the result

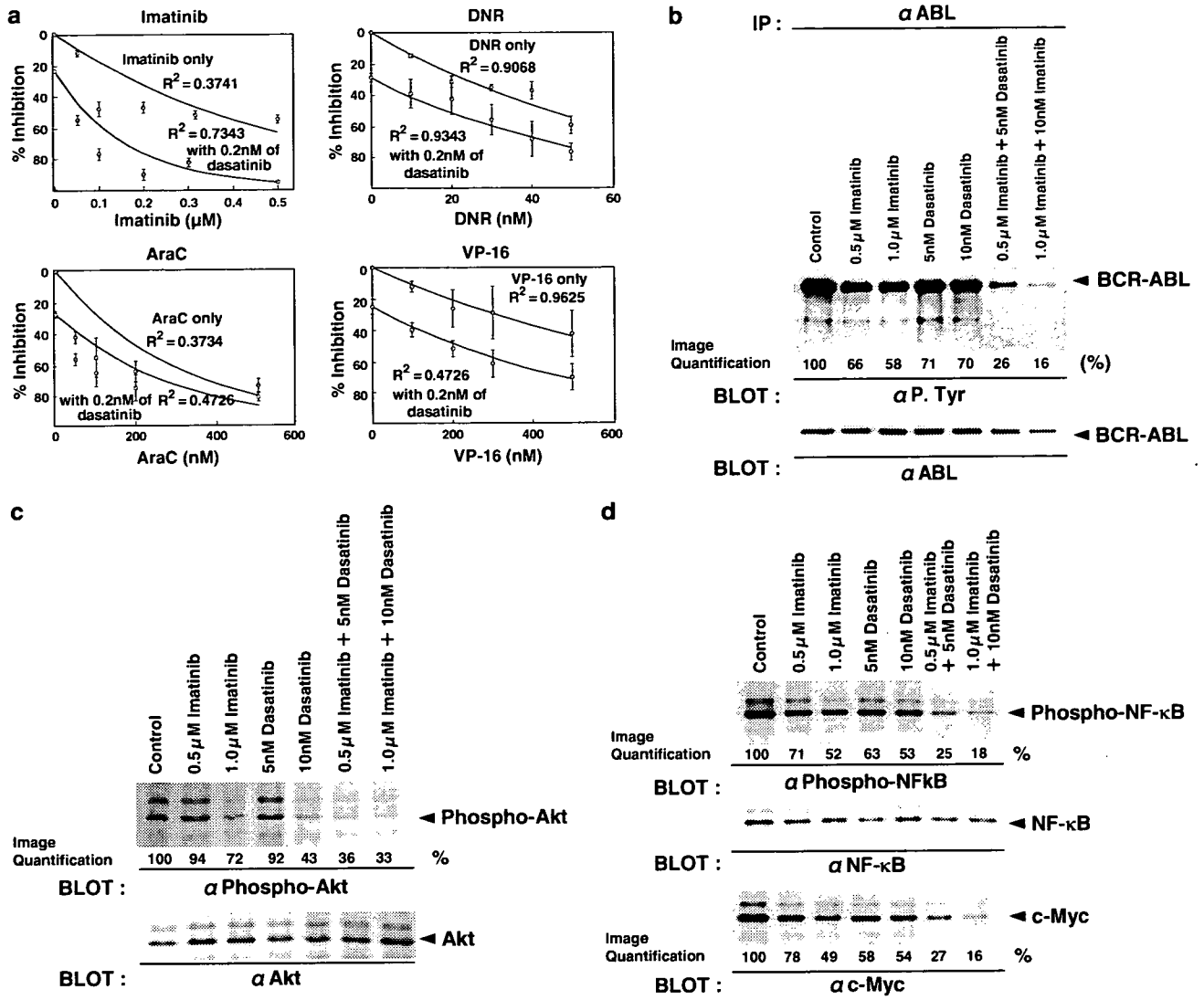

Figure 1 Analysis of combined drug effects. (**a**) K562 cells were suspended to a final concentration of 1×10^5 cells/ml in fresh medium, and incubated with anti-leukemic agents alone or in combination with 0.2 nM of dasatinib at 37°C for 72 h. The number of cells in each well was counted by flow cytometry. Regression lines generated by Microsoft Excel represent the best-fit relationship between drug concentration and the percentage inhibition of proliferation. R^2 values are the square of the correlation coefficient. Similar results were obtained in each of three separate experiments. (**b**) K562 cells were cultured with indicated concentrations of dasatinib or imatinib for 24 h, and cell lysates were immunoprecipitated with ant-ABL mAb. The immunoprecipitates were immunoblotted with anti-phosphotyrosine mAb (PY20) or anti-ABL Ab. (**c**) K562 cells were cultured with indicated concentrations of dasatinib or imatinib for 24 h, and the cell lysates were immunoblotted with anti-phospho-Akt or anti-Akt Ab. (**d**) K562 cells were cultured with indicated concentrations of dasatinib or imatinib for 24 h, and the cell lysates were immunoblotted with anti-phospho-NF-κB, anti-NF-κB or anti-c-Myc Ab.

of chain reactions of transcriptional inactivation. For instance, *CCD2* is known to be directly regulated by *MYC* at transcriptional sites, and its downregulation is logically linked to downregulated *MYC* (Figure 3a).

Oncogenic signals genes

Inactivation of BCR-ABL tyrosine kinase by dasatinib or imatinib blocks the transcription factors, and thus represses expression of target genes such as those encoding signal transduction molecules, as highlighted by members of STAT pathway (*STAT1*, *STAT3*, *STAT4*, *STAT5A*, *STAT5B* and *STAT6*) (Figure 3c).

Apoptosis-related genes

The intrinsic apoptotic pathway is important for dasatinib- or imatinib-mediated apoptosis. Both ABL kinase inhibitors modulated the expression of many genes that play a key role in this pathway, such as *BAX*, *BAK1*, *BID*, *BCL2*, *BCL6*, *BCL9*, *MCL1*, *CASP1*, *CASP2*, *CASP3*, *CASP6*, *CASP7* *CASP8*, *CASP9* and *CASP10* (Figure 4a). Moreover, genes that regulate the induction or prolongation of this pathway, including NF-κB-pathway genes (*NF-κB1* and *NF-κB1A*), were also transcriptionally reduced (Figure 4b). *GADD45B*, which induces cell cycle arrest at G2/M, was also reduced by dasatinib and imatinib (Figure 4b).

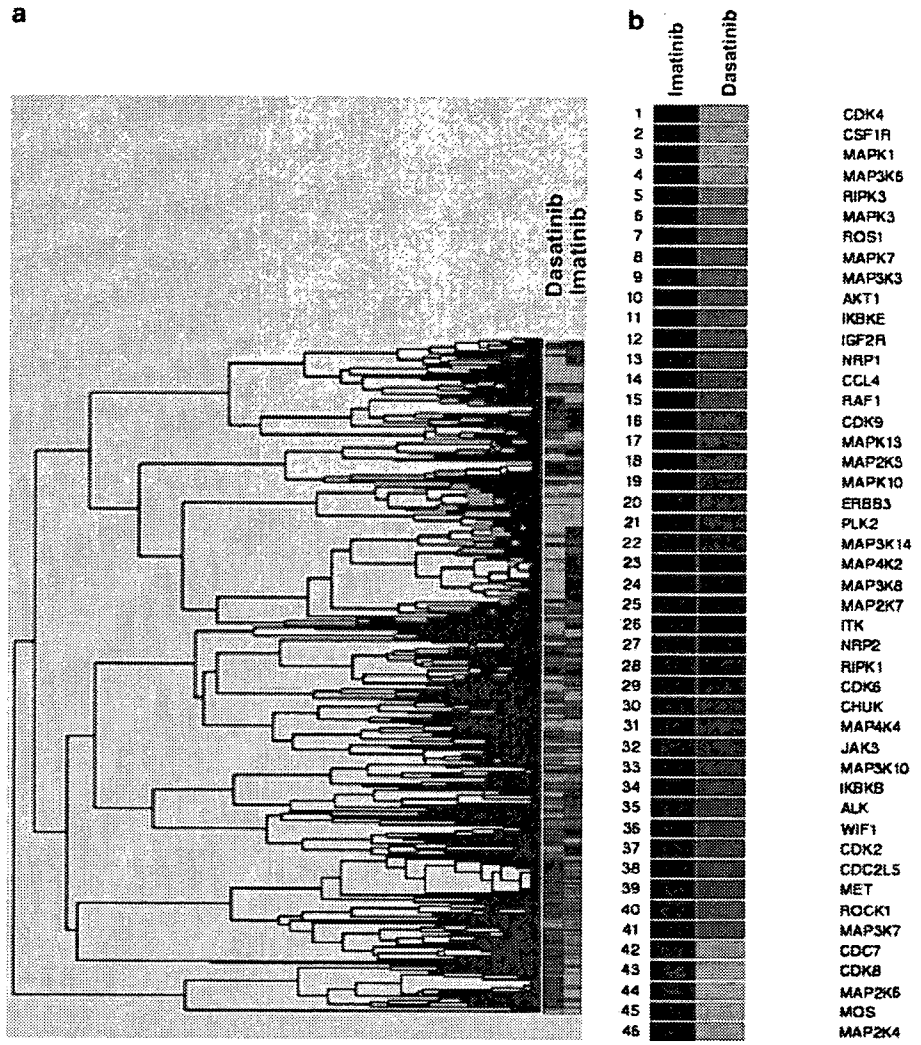

Figure 2 Hierarchical cluster analysis of gene expression profiles induced by dasatinib or imatinib in K562 cells. (**a** and **b**) K562 cells were cultured with 100 nM of dasatinib or 5 μM of imatinib for 16 h, and gene expression data from three-independent microarray hybridizations were analysed (GPL 2523). The microarray experiment data were deposited in GEO (GSE 2810). The scale in this figure shows the level of expression, where red indicates increased gene expression, green indicates decreased expression, and the intensity of color correlated to the magnitude changes. Black indicates no change.

Furthermore, genes coding tumor necrosis factor (TNF) family receptors and ligands (*TNF*, *TNFAIP3*, *TNFRSR5* and *TNFRSF12*) were activated by dasatinib or imatinib (Figure 4b).

DNA-damage repair genes

BCR-ABL-transformed cells appeared to be better equipped to survive genotoxic damage because of enhanced ability to repair DNA lesions, prolonged activation of the G/2M checkpoint to provide more time for repair, and inhibited apoptosis mechanisms. Dasatinib and imatinib reduced the expression of several DNA-damage repair pathway genes, such as *RAD50*, *RAD51L3*, *RECQL*, *XRCC1*, *XRCC3* and *XRCC4* (Figure 4c). Diverse modulation of these DNA-damage repair genes by both ABL kinase inhibitors may participate in the reduced possibility of therapeutic drug resistance.

Validation of expression profiles of selected genes

To verify the changes of CDKs expression, which were identified as selectively altered by either dasatinib or imatinib, we performed the immunoblot analysis focusing on CDK2, CDK3, CDK4, CDK6, CDK8 and CDK9 (Figure 5a). K562 cells were cultured with indicated concentrations of either dasatinib or imatinib for 48 h, and the cell lysates were immunoblotted with the indicated antibodies (Figure 5a). Protein expressions of CDK2 and CDK8 were selectively reduced by dasatinib treatment (Figure 5a). Quantitative real-time PCR analysis of these CDKs confirmed that protein expression changes induced by dasatinib and imatinib correlated with changes in gene expression (data not shown). We also determined the protein expression of CDK2 and CDK8 in TF-1-BCR-ABL cells after dasatinib or imatinib treatment (Figure 5b). Expressions of CDK2 and CDK8 was mainly reduced by dasatinib-treatment (Figure 5b). As caspase-3 activity might affect the

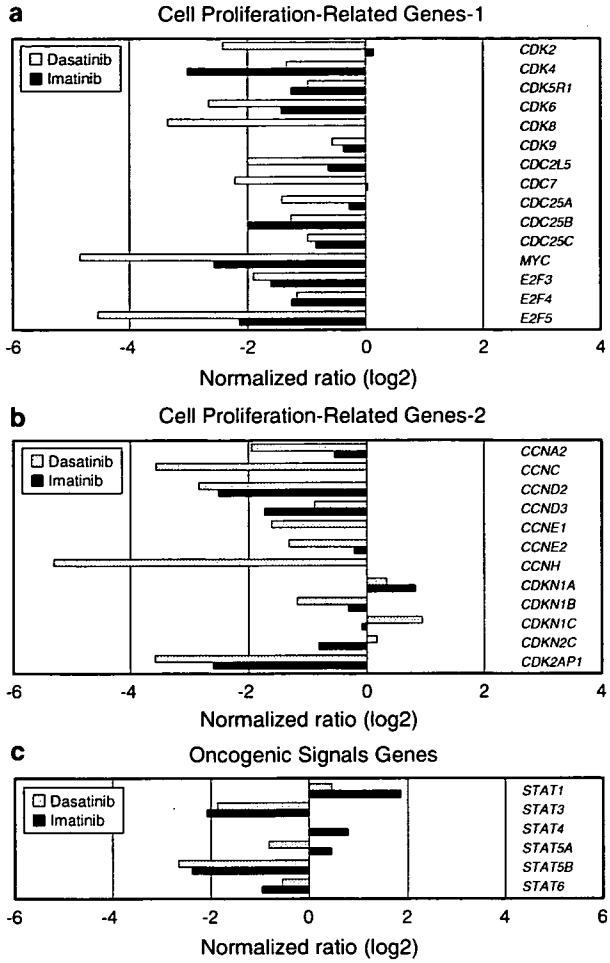

Figure 3 Dasatinib- and imatinib-regulated cell proliferation genes and STAT family genes. (**a**) Genes encode members of cyclin-dependent kinases, cell division cycle genes, c-myc and E2F family. (**b**) Genes encode members of cyclins, mitotic inhibitors. (**c**) Genes encode members of *STAT* family.

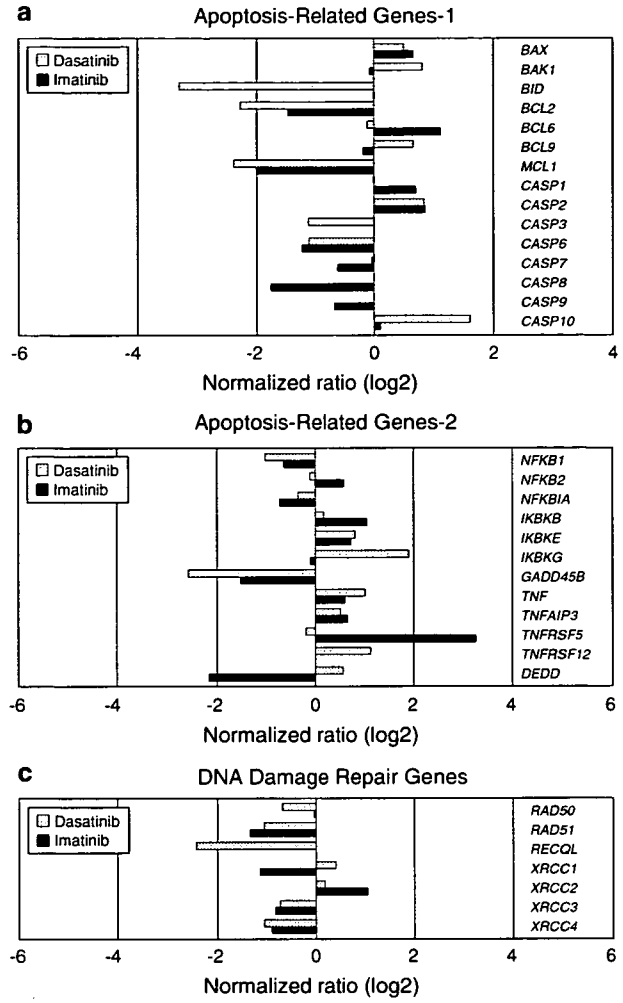

Figure 4 Dasatinib- and imatinib-regulated apoptosis genes and DNA-damage repair genes. (**a** and **b**) Genes encode members of apoptotic proteins. (**c**) Genes encode members of *NF-κB* pathways and the death receptor pathway.

reduction of CDK2 or CDK8, therefore, we determined the time-dependent changes of CDK2/CDK8 expression and caspase-3 and poly(ADP-ribose)polymerase (PARP) activation in K562 cells (Figure 5c and d). K562 cells were cultured with either 100 nM of dasatinib or 10 μM of imatinib for the indicated time, and the cell lysates were immunoblotted with indicated antibodies (Figure 5c and d). The expression of CDK2 or CDK8 proteins was reduced after 24 h of dasatinib treatment (Figure 5c); however, the expression of CDK2 or CDK8 proteins was nearly unchanged after imatinib treatment (Figure 5d). As activation of caspase-3 or PARP was observed 12–24 h after dasatinib or imatinib treatment (Figure 5c and d), it is likely that caspase-3 activity may not be required for the reduction of CDK2/CDK8 protein level.

siRNA-mediated knock down of CDK2 *and* CDK8 *in K562 cells and TF-1BCR-ABL cells*

To assess the functional importance of dasatinib- and imatinib-regulated gene, we used RNA interference to determine whether reduction in *CDK2* and *CDK8* affect the proliferation. K562 and TF-1BCR-ABL cells were transfected with control siRNA or *CDK2* siRNA or *CDK8* siRNA; then the CDK2 and CDK8 expression was analysed by immunoblotting after 48 h (Figure 6a). The siRNA to *CDK2* or *CDK8* specifically reduced CDK2 or CDK8 expression (Figure 6a). At 48 h after transfection, K562 and TF-1BCR-ABL cells were treated with the indicated concentration of dasatinib or imatinib for 48 h, and viable cells were counted (Figure 6b and c). Increasing doses of imatinib, in the presence of *CDK2* siRNA or *CDK8* siRNA, shifted the dose–response curve substantially downward, consistent with increased antiproliferative activity (Figure 6b and c). When dasatinib was treated in the presence of *CDK2* siRNA or *CDK8* siRNA, the two curves crossed at 200 nM of dasatinib (Figure 6b and c). These results demonstrated that transcriptional repression of *CDK2* or *CDK8* can play an important role in the combined growth inhibitory effects of dasatinib and imatinib.

Discussion

Imatinib and dasatinib are clinically active ABL tyrosine kinase inhibitors that show the additive/synergistic growth inhibition on BCR-ABL-expressing cells (Figure 1a). Earlier studies demonstrated that dasatinib and imatinib largely activated common apoptotic pathways, although there were differences in the activities of the two compounds. Dasatinib is capable of binding BCR-ABL with less stringent conformational requirements with respect to imatinib (Gambacorti-Passerini *et al*., 2005). Although both compounds inhibit

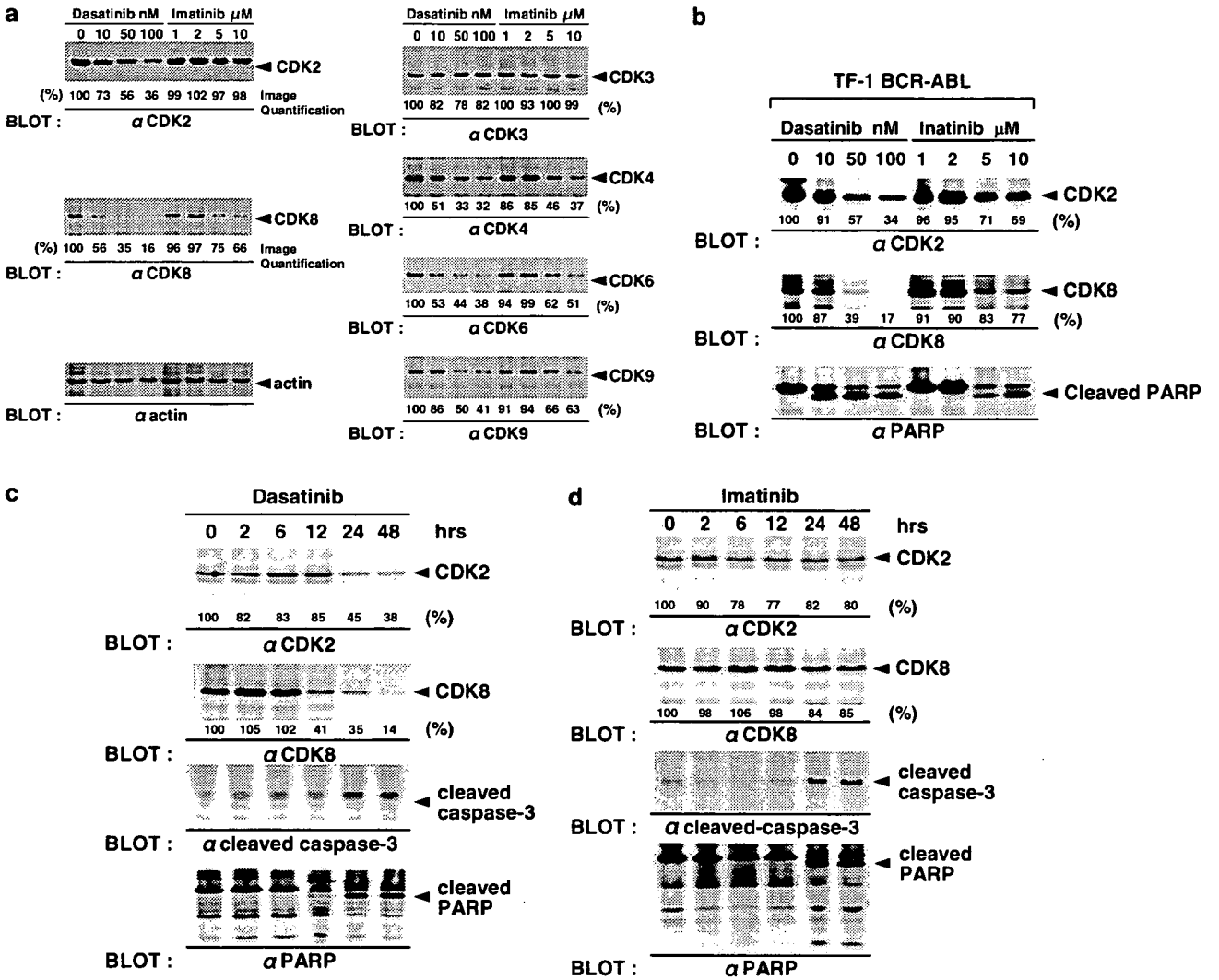

Figure 5 Validation of microarray data of cyclin-dependent kinase genes. (**a**) K562 cells were cultured with indicated concentrations of either dasatinib or imatinib for 48 h, and the cell lysates were immunoblotted with the indicated antibodies. Quantitative analysis of CDK2 and CDK8 expression was carried out by analysing hyper-ECL films of immunoblotting by using a densitometer. (**b**) TF-1BCR-ABL cells were cultured with indicated concentrations of dasatinib or imatinib for 48 h, and the cell lysates were immunoblotted with anti-CDK2 or anti-CDK8 or anti-PARP Ab. (**c** and **d**) K562 cells were cultured with either 100 nM of dasatinib (**c**) or 10 μM of imatinib (**d**) for the indicated time, and the cell lysates were immunoblotted with anti-CDK2, anti-CDK8 or anti-cleaved caspase-3, or anti-PARP Ab.

Figure 6 Knock down of CDK2 and CDK8 expression affected the proliferation in dasatinib- or imatinib-treated K562 cells and TF-1BCR-ABL cells. (**a**) K562 cells and TF-1BCR-ABL cells transfected with 1.25 μM of control (GFP), or *CDK2* siRNA or *CDK8* siRNA were analysed 48 h after transfection for CDK2 or CDK8 expression by immunoblotting. (**b** and **c**) At 48 h after transfection, K562 (**b**) and TF-1BCR-ABL cells (**c**) were treated with incubated concentrations of dasatinib or imatinib for 48 h; viable cells were counted by using a Vi-cell XR automated cell viability analyzer (Beckman Coulter). The mean number of viable cells at different concentrations of drug was normalized to the mean number of viable cells in the no-drug sample. Similar results were obtained in each of three independent experiments.

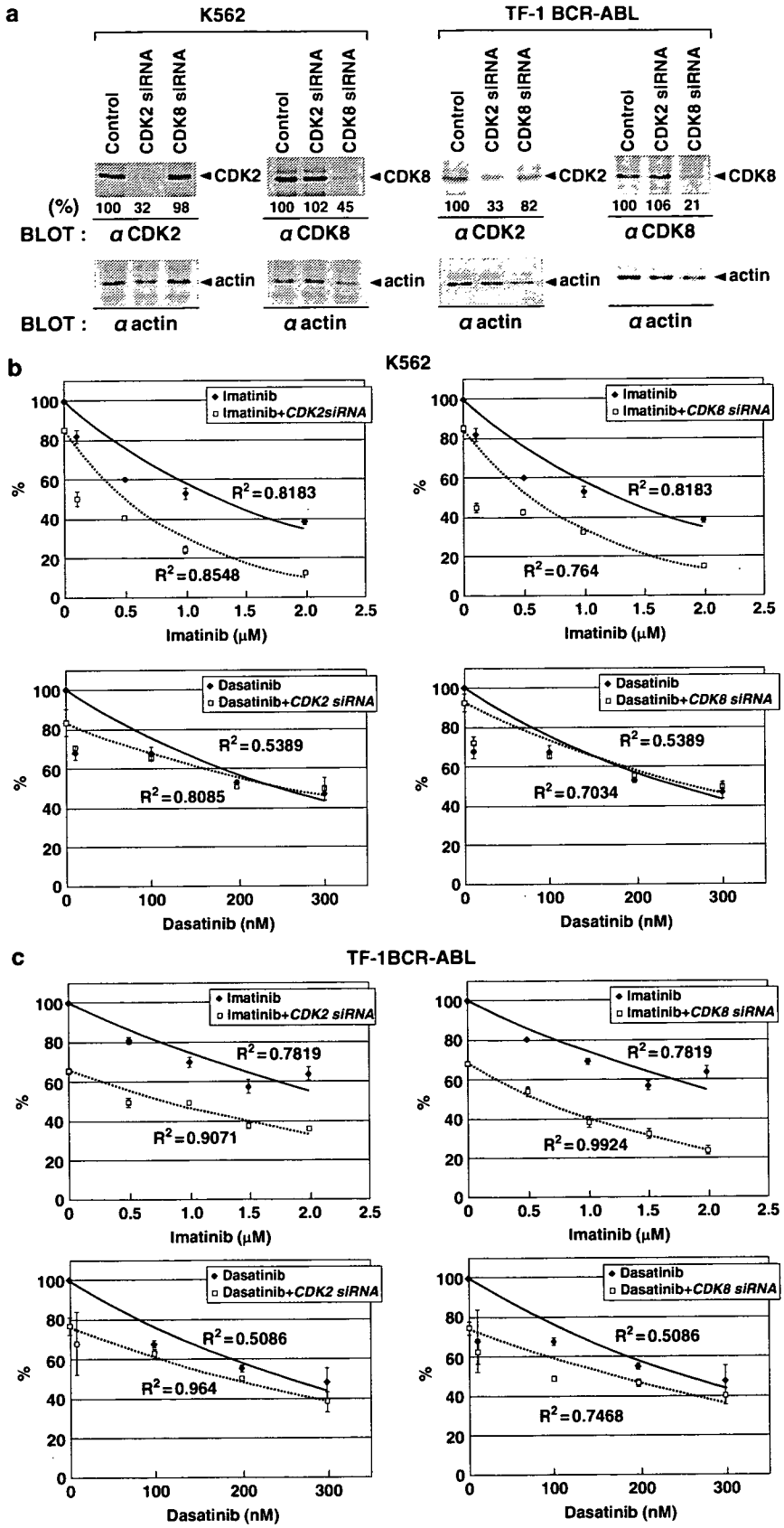
a
K562
TF-1 BCR-ABL
Control
CDK2 siRNA
CDK8 siRNA
CDK2
CDK8
(%) 100 32 98
100 102 45
100 33 82
100 106 21
BLOT : α CDK2
α CDK8
actin
α actin
b
K562
Imatinib
Imatinib+CDK2siRNA
Imatinib+CDK8 siRNA
R²=0.8183
R²=0.8548
R²=0.764
Imatinib (μM)
Dasatinib
Dasatinib+CDK2 siRNA
Dasatinib+CDK8 siRNA
R²=0.5389
R²=0.8085
R²=0.7034
Dasatinib (nM)
c
TF-1BCR-ABL
R²=0.7819
R²=0.9071
R²=0.9924
R²=0.5086
R²=0.964
R²=0.7468

BCR-ABL tyrosine kinase, whether these two structurally diverse compounds mediate similar or disparate gene expression changes has not been addressed. In the present study, we used microarray gene expression profiles to identify the genes commonly and selectively regulated by dasatinib and imatinib.

On the basis of clustering, the transcriptional responses induced by dasatinib and imatinib were remarkably similar (Figure 2a). Some degree of overlap was expected because both compounds target BCR-ABL kinase. Compatible with this phenotype, some proapoptotic genes were upregulated, a number of antiapoptotic genes were downregulated by both ABL kinase inhibitors, and a number of genes within the same molecular pathway were coordinately regulated (Figures 3 and 4). These include *BAX*, *BCL-2*, *MCL-1*, *CASP2* and *CASP10* (Figure 4a). Although some of the proapoptotic genes were repressed (i.e., *BID*, *CASP3* and *CASP6*), the overall response was one that would provide a strong proapoptotic signal (Figure 4a and b). Moreover, repression of the NF-κB pathway is also associated with apoptotic stimulus (Figure 4b). Furthermore, the transcription of TNF superfamily genes and genes involved in death-receptor signaling (DEDD) was altered by dasatinib or imatinib (Figure 4b).

In addition to inducing apoptosis, ABL kinase inhibitors can suppress cell cycle progression (Gesbert *et al.*, 2000; Parada *et al.*, 2001). The transcriptional response was consistent with growth suppression, and a number of genes within key growth-regulatory pathways were coordinately regulated (Figure 3a and b). For example, decreased expression of *MYC*, *E2F3*, *E2F4* and *E2F5* is consistent with suppression of the *MYC* pathway (Figure 3a). The number of *CDKs* and *CDK* inhibitors, whose expression is highly coordinated to regulate appropriate cell cycle progression, was aberrantly expressed in dasatinib- or imatinib-treated cells (Figure 3b). *CDK2* and *CDK8* are selectively modulated by dasatinib, which had a maximal reduction of <5-fold in microarray screen (Figure 3a). We have shown that dasatinib and imatinib and the combination of these compounds differently suppress the expression of c-Myc protein (Figure 1d). Recently, Samanta *et al.* (2006) demonstrated that signal transduction by BCR-ABL/Jak2 network results in phosphorylation of Akt, which leads to the stabilization of c-Myc and activates NF-κB to cause elevation of c-Myc transcripts. As compared with treatment with either agent alone, co-treatment with dasatinib and imatinib caused more attenuation of the levels of phospho-Akt, phospho-NFκB and c-Myc (Figure 1c and d).

As CDK2 is a c-Myc transcriptional target (Prathapam *et al.*, 2006), downregulation of a large number of cell cycle-related genes, including CDK2 and CDK8, could be largely the result of chain reactions of transcriptional inactivation by these ABL tyrosine kinase inhibitors. Earlier study (Riley *et al.*, 2001) demonstrated that v-SRC induces the expression of CDK2 in Rat-1 cells. Therefore, inactivation of c-SRC and SRC-family kinase by dasatinib may decrease the expression of CDK2. Progression through the cell cycle from G1 to S phase requires sequential activation of CDK2 and CDK4 (Sherr and Roberts, 1999). The role of CDK4 is well established; however, CDK2 may be regulated differently in somatic cells and in cancer cells (Tetsu and McCormick, 2003). In BCR-ABL-transformed cells, cyclin D activates CDK4/CDK6, which inturn transactivates cyclin E by releasing E2F. Cyclin E activates CDK2, and BCR-ABL causes relocation of p27 to the cytoplasm, further stimulating CDK2 (Jiang *et al.*, 2000). Therefore, CDK2 seems to have a critical role in cell cycle progression in BCR-ABL-transformed cells. Downregulation of *CDK2* or *CDK8* by siRNA increased antiproliferative activity in imatinib-treated cells, but not in dasatinib-treated cells (Figure 6a–c). Our results clearly demonstrate that diverse regulation of *CDKs* by ABL kinase inhibitors may contribute at least in part to additive growth inhibition in these compounds. The pleiotropic molecular sequel of SRC/ABL inhibition does not allow us to conclude which pathways are most important for anti-tumor effect, but potentially offer a major therapeutic advantage, namely the simultaneous targeting of different proliferative/antiapoptotic pathways in tumor cells (Supplementary Figure).

One of the objectives of this study of the molecular profile of dasatinib-treated BCR-ABL-transformed cells was to establish a framework for designing of combination therapies with conventional anti-leukemia agents. This study identified the enhanced antiproliferative activity of combinations with dasatinib with anti-leukemia agents, such as imatinib, daunorubicine and VP-16 (Figure 1a). The ability of dasatinib to suppress genes involved in cell proliferation-related genes (i.e., *CDK2*, *CDK6*, *CDK8*, *CDC7*, *CCNA2*, *CCNC*, *CCNE1*, *CCNE2* and *MYC*) and antiapoptotic genes (*BCL2*, *MCL1* and *NFκB*) superior to imatinib constitute a molecular basis for the chemo-sensitizing effect of SRC/ABL kinase inhibition.

This study provides comparative gene expression profiling analysis of the effect of dasatinib and imatinib, two compounds that are clinically active for BCR-ABL-positive leukemia. Both agents commonly target a number of important molecular pathways that regulate cell growth and survival. A single proapoptotic or antiproliferative pathway may not be critical for the therapeutic effects of ABL kinase inhibitors. The present findings have important implications for the clinical use of dasatinib and imatinib as an anti-leukemia agent, either alone or in combination with other agents.

Materials and methods

Antibodies and reagents

Anti-CDK2 Ab (D-12), anti-CDK3 Ab (Y-20), anti-CDK4 Ab (H-22), anti-CDK6 Ab (C-21), anti-CDK8 Ab (D-9), anti-CDK9 Ab (C-20), anti-actin Ab (C-2) and anti-ABL Ab (24-11) were purchased from Santa Cruz Biotechnology, Inc. (Santa Cruz, CA, USA). Antiphosphotyrosine mAb (PY20) was purchased from Becton Dickinson and Company (Franklin Lakes, NJ, USA). Anti-Akt Ab, anti-phospho-Akt (Ser473)

Ab, anti-NF-κB p65 Ab and anti-phospho-NF-κB p65 (Ser536) Ab were purchased from Cell Signaling (Beverly, MA, USA). Anti-c-Myc Ab was purchased from NOVUS (Littleton, CO, USA). Dasatinib was kindly provided by Bristol-Myers Squibb (New York, NY, USA). DNR, cytosine arabinoside (Ara C) and etoposide (VP-16) were obtained from Sigma (St Louis, MO, USA).

Cells and cell culture

K562 cells were obtained from the American Type Culture Collection (Rockville, MD, USA). TF-1BCR-ABL cells were described previously (Komatsu *et al.*, 2003). These cell lines were cultured in RPMI1640 (Life Technology Inc., Rockville, MD, USA), supplemented with 10% FCS (Hyclone Laboratories, Logan, UT, USA).

Analysis of combined drug effects

K562 cells were suspended to a final concentration of 1×10^5 cells/ml in fresh medium, plated in 24-well dishes and incubated with anti-leukemic agents alone or in combination with 0.2 nM of dasatinib at 37°C for 72 h. The anti-leukemic agents used were imatinib, DNR, AraC or VP16. The number of cells in each well was counted by flow cytometry, and the cell numbers were normalized by dividing the number of cells in the absence of anti-leukemic agents or with dasatinib alone. The data were plotted as the concentration of anti-leukemic agents against the percentage inhibition of proliferation. To determine the relationship between the percentage inhibition of proliferation and drug concentration, a best-fit regression line was generated by Microsoft Excel.

Oligonucleotide DNA microarray hybridization

We have designed two types of pathway focusing on low-density oligonucleotide microarrays (Novusgene Inc., Tokyo, Japan), which contain 667 selected genes related to cell growth, cell cycle, apoptosis, transcription, DNA repair and cell stress responses (GEO accession number: GPL2523). This DNA chip was made up of tetra-plicate spots of 60-mer highly specific oligonucleotide probes. For DNA microarray analysis of genes, we used 1 μg of mRNA from K562 cells treated with dasatinib or imatinib for 16 h. Hybridization was carried out automatically using Gene TAC Hybridization (Genomic Solution, Ann Arbor, MI, USA) according to the supplier's instructions. The conditions of hybridization were 55°C for 2 h, 50°C for 2 h and 46°C for 2 h, then 42°C for 12 h.

Data analysis and statistic validation

The hybridization signals were scanned by GenePix 4000B Microarray Scanner (Axon Instruments, Union City, CA, USA) as raw data. The scanned data were normalized, verified and analysed using the Genomic Profiler software (Mitsui Knowledge Industry, Tokyo, Japan) as described previously (Ohyashiki *et al.*, 2005; Takaku *et al.*, 2005; Zhang *et al.*, 2006). First, the value was adjusted by subtraction of background fluorescence of an equivalent area. Analysis was carried out by taking the median signal of the probe value for each transcription set, and the 75% rank for the total hybridization was calculated. Microarray data obtained from three independent experiments were then verified in a single file. The normalized log data of fluorescence ratio (Cy5–Cy3) which was quantified for each gene to reflect the relative abundance of gene in each experimental sample compared with reference sample, were deposited with GEO. For statistical analysis of host gene expression, we also utilized a GeneSifter (VizXLabs, Seattle, WA, USA). Analysis of variance, and Student's *t*-test were performed using GeneSifter. Values of $P<0.05$ were considered to indicate a statistically significant difference, and the Benjamini–Hochberg algorithm was used for estimation of false discovery rates.

Immunoblotting and immunoprecipitation

Immunoblotting and immunoprecipitation were performed as described previously (Tauchi *et al.*, 1994). Quantitative analysis of CDK2 and CDK8 expression was carried out by analysing hyper-enhanced chemiluminescence (ECL) films of immunoblotting by using a densitometer (Bio-Rad, Hercules, CA, USA).

Small interfering RNA experiments

siRNA oligonucleotides for *CDK2* and *CDK8* were purchased from Santa Cruz Biotechnology Inc. (Santa Cruz, CA, USA), and resuspended in RNase-free H_2O at 20 μM. siRNA (1.25 μM) was added to prechilled 0.4 cm-gap electroporation cuvettes (Bio-Rad). K562 (5×10^6) or TF-1BCR-ABL cells (5×10^6) were washed twice in serum-free media and resuspended to 5×10^6 cells per 250 μl of cold, serum-free RPMI 1640. Cells were added to the cuvettes, mixed, and further mixed for 5 min on ice. Cells were then pulsed once at 250 mV, 960 μF and 200 Ω by using a Bio-Rad electroporator. At 48 h after electroporation, protein knock down was determined by immunoblotting, cells were treated with the indicated concentration of dasatinib or imatinib for 48 h, and viable cells were counted by using a Vi-cell XR automated cell viability analyzer (Beckman Coulter, Fullerton, CA, USA). The mean number of viable cells at different concentrations of drug was normalized to the mean number of viable cells in the no-drug sample.

References

Burgess MR, Skaggs BJ, Shah NP, Lee FY, Sawyers CL. (2005). Comparative analysis of two clinically active BCR-ABL kinase inhibitors reveals the role of conformation-specific binding in resistance. *Proc Natl Acad Sci USA* **102**: 3395–3400.

Dai Y, Rahmani M, Corey SJ, Dent P, Grant S. (2004). A BCR/ABL-independent, Lyn-dependent form of imatinib mesylate (STI-571) resistance is associated with altered expression of Bcl-2. *J Biol Chem* **279**: 34227–34239.

Donato NJ, Wu JY, Stapley J, Gallick G, Lin H, Arlinghaus R *et al.* (2003). BCR-ABL independent and LYN kinase overexpression in chronic myelogenous leukemia cells selected for resistance to STI571. *Blood* **101**: 690–698.

Gambacorti-Passerini C, Gasser M, Ahmed S, Assouline S, Scapozza L. (2005). Abl inhibitor BMS354825 binding mode in Abelson kinase revealed by molecular docking studies. *Leukemia* **19**: 1267–1269.

Gesbert F, Sellers WR, Signoretti S, Loda M, Griffin GD. (2000). BCR/ABL regulates expression of the cyclin-dependent kinase inhibitor p27Kip1 through the phosphatidylinositol 3-kinase/AKT pathway. *J Biol Chem* **275**: 39223–39230.

Hofmann WK, de Vos S, Elashoff D, Gschaidmeier H, Hoelzer D, Koeffler HP *et al.* (2002). Relation between resistance of Philadelphia-chromosome-positive acute lymphoblastic leukemia to the tyrosine kinase inhibitor STI571 and gene-expression profiles: a gene expression study. *Lancet* **359**: 481–486.

Jiang Y, Zhao RC, Verfaillie CM. (2000). Abnormal integrin-mediated regulation of chronic myelogenous leukemia CD34+ cell proliferation: BCR/ABL up-regulates the cyclin-dependent kinase inhibitor, p27Kip, which is relocated to the cell cytoplasm and incapable of regulating cdk2 activity. *Proc Natl Acad Sci USA* **97**: 10538–10543.

Komatsu N, Watanabe T, Uchida M, Mori M, Kirito K, Kikuchi S *et al.* (2003). A member of Forkhead transcription factor FKHRL1 is a downstream effector of STI571-induced cell cycle arrest in BCR-ABL-expressing cells. *J Biol Chem* **278**: 6411–6419.

Lionberger JM, Wilson MB, Smithgall TE. (2000). Transformation of myeloid leukemia cells to cytokine independence by BCR-ABL is suppressed by kinase-defective Hck. *J Biol Chem* **275**: 18581–18585.

Nakajima A, Tauchi T, Sumi M, Bishop WR, Ohyashiki K. (2003). Efficacy of SCH66336, a farnesyl transferase inhibitor, in conjunction with imatinib against BCR-ABL-positive cells. *Mol Cancer Ther* **2**: 219–224.

O'Hare T, Walters DK, Stoffregen EP, Jia T, Manley PW, Mestan J *et al.* (2005). *In vitro* activity of BCR-ABL inhibitors AMN107 and BMS-354825 against clinically relevant imatinib-resistant Abl kinase domain mutants. *Cancer Res* **65**: 4500–4505.

Ohyashiki JH, Takaku T, Ojima T, Abe K, Yamamoto K, Zhang Y *et al.* (2005). Transcriptional profiling of human herpesvirus type B (HHV-6B) in an adult T cell leukemia cell line as *in vitro* model for persistent infection. *Biochem Biophys Res Commun* **329**: 11–17.

Parada Y, Banerji L, Glassford J, Lea NC, Collada M, Rivas C *et al.* (2001). BCR-ABL and interleukin 3 promote haematopoietic cell proliferation and survival through modulation of cyclin D2 and p27Kip1 expression. *J Biol Chem* **276**: 23572–23580.

Prathapam T, Tegen S, Oskarsson T, Trumpp A, Martin GS. (2006). Activated Src abrogates the Myc requirement for the G0/G1 transition but not for the G1/S transition. *Proc Natl Acad Sci USA* **103**: 2695–2700.

Ptasznik A, Nakata Y, Kalota A, Emerson SG, Gewirtz AM. (2004). Short interfering RNA (siRNA) targeting the Lyn kinase induces apoptosis in primary, and drug-resistant, BCR-ABL1(+) leukemia cells. *Nat. Med* **10**: 1187–1189.

Riley D, Carragher NO, Frame MC, Wyke JA. (2001). The mechanism of cell cycle regulation by v-Src. *Oncogene* **20**: 5941–5950.

Samanta AK, Lin H, Sun T, Kantarjian H, Arlinghaus RB. (2006). Janus kinase 2: a critical target in chronic myelogenous leukemia. *Cancer Res* **66**: 6468–6472.

Shah NP, Tran C, Lee FY, Chen P, Norris D, Sawyers CL. (2004). Overriding imatinib resistance with a novel ABL kinase inhibitor. *Science* **305**: 399–401.

Sherr CJ, Roberts JM. (1999). CDK inhibitors: positive and negative regulators of G1-phase progression. *Genes Dev* **13**: 1501–1512.

Stanglmaier M, Warmuth M, Kleinlein I, Hallek M. (2003). The interaction of the BCR-ABL tyrosine kinase Hck is mediated by multiple binding domains. *Leukemia* **17**: 286–289.

Takaku T, Ohyashiki JH, Zhang Y, Ohyashiki K. (2005). Estimating immunoregulatory gene networks in human herpesvirus type 6-infected T cells. *Biochem Biophys Res Commu* **336**: 469–477.

Talpaz M, Shah NP, Kantarjian H, Donato N, Nicoll J, Paquette R *et al.* (2006). Dasatinib in imatinib-resistant Philadelphia chromosome-positive leukemias. *N Engl J Med* **354**: 2531–2541.

Tauchi T, Feng GS, Shen R, Song HY, Donner D, Pawson T *et al.* (1994). SH2-containing phosphotyrosine phosphatase Syp is a target of p210bcr-abl tyrosine kinase. *J Biol Chem* **269**: 15381–15387.

Tetsu O, McCormick F. (2003). Proliferation of cancer cells despite CDK2 inhibition. *Cancer Cell* **3**: 233–245.

Thomas SM, Brugge JS. (1997). Cellular functions regulated by Src family kinases. *Annu Rev Cell Dev Biol* **13**: 513–609.

Warmuth M, Bergmann M, Priess A, Hauslmann K, Emmerich B, Hallek M. (1997). The Src family kinase Hck interacts with BCR-ABL by a kinase-independent mechanism and phosphorylates the Grb2-binding site of BCR. *J Biol Chem* **272**: 33260–33270.

Zhang Y, Ohyashiki JH, Takaku T, Shimizu N, Ohyashiki K. (2006). Transcriptional profiling of Epstein–Barr virus (EBV) genes and host cellular genes in nasal NK/T-cell lymphoma and chronic active EBV infection. *Br J Cancer* **94**: 599–608.

Supplementary Information accompanies the paper on the Oncogene website (http://www.nature.com/onc).

STEM CELLS AND DEVELOPMENT 16:503–514 (2007)

DOI: 10.1089/scd.2007.9994

Original Research Report

Depsipeptide (FK228) Preferentially Induces Apoptosis in BCR/ABL-Expressing Cell Lines and Cells from Patients with Chronic Myelogenous Leukemia in Blast Crisis

SEIICHI OKABE,[1] TETSUZO TAUCHI,[1] AKIHIRO NAKAJIMA,[1] GORO SASHIDA,[1] AKIHIKO GOTOH,[1] HAL E. BROXMEYER,[2] JUNKO H. OHYASHIKI,[3] and KAZUMA OHYASHIKI[1]

ABSTRACT

Resistance to imatinib can occur in patients with chronic myelogenous leukemia (CML). In this study, we report mechanisms of action of histone deacetylase (HDAC) inhibitor, depsipeptide (FK228) in BCR/ABL-expressing cell lines and its effectiveness in imatinib-resistant cells from patients with blast crisis of CML. FK228 potently induced apoptosis of TF-1 BCR/ABL, K562, and H7 BCR/ABL cells. We found that histone H4, BCR/ABL, heat shock protein 90 (HSP-90), p53, focal adhesion kinase (FAK), paxillin, and retinoblastoma protein (Rb) were acetylated in the treated cells. Cells were also blocked in G_2/M phase of the cell cycle and activity of mitogen-activated protein kinase (MAPK) was blocked, but p38MAPK (p38) was activated. Inhibitor of apoptosis proteins (IAPs) were suppressed, and common results of apoptotic induction were observed, such as caspase-3, caspase-9, and poly(ADP-ribose) polymerase (PARP) activation. Although p38 was phosphorylated after FK228 treatment, histone H4 acetylation, caspase-3 activation, and apoptosis were not inhibited by treatment with the p38 inhibitor SB203580. We also found that human telomerase reverse transcriptase (hTERT) ShRNA-transfected cells demonstrated decreased FK228-induced apoptosis. Of clinical relevance, FK228-induced apoptosis of imatinib-resistant primary cells from patients with CML, who had progressed to blast crisis (BC) while receiving therapy with imatinib. In conclusion, FK228 potently induces apoptosis of CML cells by acetylation and degradation of BCR/ABL protein. Our study suggests how FK228 may mediate its effects on imatinib-resistant CML cells.

INTRODUCTION

THE SELECTIVE TYROSINE KINASE INHIBITOR imatinib is increasingly used for treatment of Philadelphia chromosome-positive leukemias and other malignancies. Imatinib has shown remarkable clinical activity in patients with chronic myelogenous leukaemia (CML) (1). However, the emergence of resistance to imatinib remains a major problem in the treatment of CML. In particular, development of resistance to imatinib is a frequent problem in treatment of patients in advanced phases of CML. Several mechanisms of resistance have been described, the most frequent of which are amplification and/or mutations of the BCR/ABL gene. Mutations in the kinase domain (KD) of BCR/ABL impairs binding of imatinib and causes resistance to imatinib (2). Therefore, alternative or additional

[1]First Department of Internal Medicine, Tokyo Medical University, Tokyo, Japan.
[2]Department of Microbiology and Immunology, and the Walther Oncology Center, Indiana University School of Medicine, Indianapolis, IN 46202.
[3]Intractable Disease Research Center, Tokyo Medical University, Tokyo, Japan.

treatment is necessary to overcome imatinib resistance in BCR/ABL-positive leukemia (3).

In eukaryotic cells, histone acetylation/deacetylation is important in transcriptional regulation. Chromatin acetylation is controlled by opposing effects of two families of enzymes: histone acetyltransferases (HAT) and histone deacetylases (HDAC) (4). It has been reported that deregulation of HDAC activity may be a cause of malignant disease in humans (5). Inhibition of HDAC regulates transcriptional activation of specific genes through relaxation of chromatin conformation, and HDAC is considered a promising target for cancer treatment (6). Because histone deacetylase inhibitors show significant activity against a broad spectrum of neoplasms, many HDAC inhibitors have entered clinical trials for both solid and liquid tumors (6,7). There are several types of HDAC inhibitors; one, depsipeptide (FK228) is produced by *Chromobacterium violaceum* (8). FK228 has potent antitumor activities; this is associated with induction of apoptosis, and cell cycle arrest (9,10). Some patients with cutaneous T cell lymphomas have manifested complete or partial responses in a phase study of FK228 at the National Cancer Institute (11). However, mechanisms of FK228-induced apoptosis in BCR/ABL-expressing cells and imatinib-resistant CML cells have not yet been fully elucidated.

The aims of this study were to clarify the mechanisms of action of FK228 in BCR/ABL-expressing cells and to determine whether depsipeptide was effective in imatinib-resistant primary cells from patients with CML.

MATERIALS AND METHODS

Reagents and antibodies

Depsipeptide (FK228) was generously provided by Exploratory Research Laboratories, Fujisawa Pharmaceutical Co. Ltd. (Tokyo, Japan). A stock solution of FK228 was dissolved in ethyl alcohol and diluted in growth medium. Anti-acetyl histone H4 antibody (Ab), and histone H4 Ab were purchased from Upstate Biotechnology (Lake Placid, NY). Anti-phospho-mitogen-activated protein kinase (MAPK), and p38 MAPK (p38) Abs, anti-cleaved caspase-9, caspase-3, poly(ADP-ribose) polymerase (PARP), and retinoblastoma (Rb) Abs were purchased from Cell Signaling (Beverly, MA). P53, Abl, focal adhesion kinase (FAK), β-tubulin, c-jun amino-terminal kinase (JNK), and phosphor-JNK Abs were obtained from Santa Cruz Biotechnology (Santa Cruz, CA). Extracellular signal-regulated kinase-1 (Erk-1), heat shock protein-90 (HSP-90), and paxillin Abs were obtained from Transduction Laboratories (Lexington, KY). Horseradish peroxidase (HRP)-conjugated acetylated Lysine Ab was obtained from Stressgen Bioreagents (Ann Arbor, MI). AntibodyArray was obtained from Hypromatrix, Inc. (Worcester, MA). Other reagents were obtained from Sigma (St Louis, MI). human telomerase reverse transcriptase (hTERT) ShRNA-expression retroviral vectors, and control vectors were generously provided by Dr. Masutomi (Harvard Medical School, MA) (12).

Cell culture, transfection, and isolation of primary CML cells

TF-1 BCR/ABL (13), K562 (which expresses BCR/ABL) and H7 BCR/ABL (14) cells were maintained in RPMI-1640 medium supplemented with 10% heat-inactivated fetal bovine serum (FBS) with 1% penicillin/streptomycin in a humidified incubator at 37°C. TF-1 cells were maintained in liquid culture with 1 ng/ml granulocyte-macrophage colony-stimulating factor (GM-CSF). K562 cells were transfected by electroporation as previously described (15). Beginning 48 h after electroporation, cells were selected with 2 μg/ml puromycin and cloned by limiting dilution. Population doubling (PD) was defined as the time at which cultures reached confluence in 10-cm culture dishes. In some experiments, blast crisis CML cells freshly isolated from a patient who was resistant to STI571 (imatinib) were used. The patient gave informed consent prior to the study. Mononuclear cells were obtained from the peripheral blood by Ficoll-Hypaque fractionation. Isolated mononuclear cells consisting of more than 80% leukemic blast cells were used.

Cell proliferation assay

Cells were plated in 96-well cell culture plates (8×10^3 cells/well) and were treated with FK228 at the indicated concentrations. Treated cells were maintained and stained with a cell counting kit solution (Dojin, Kumamoto, Japan) and measured photometrically (A595 nm) to determine cell viability.

Immunoprecipitation and western blot analysis

Immunoprecipitation and western blot analysis was as previously described (16,17).

Cell cycle analysis

Cell cycle distribution was analyzed using propidium iodide (PI)-stained cells. One hundred thousand cells were washed with phosphate-buffered saline (PBS), fixed, and stained with solution containing 1% PI, 100 μg/ml digitonin, 0.01% NaN_3, 200 μg/ml RNase